# Applications of Laser-induced Emission Spectral Analysis for Industrial Process and Quality Control*

**Claus J. Lorenzen, Christoph Carlhoff, Ulrich Hahn and Martin Jogwich**
*Krupp Forschungsinstitut GmbH, Postfach 10 22 52, D-4300 Essen 1, Germany*

Laser-induced emission spectral analysis (LIESA, a registered trademark of instruments developed by Krupp), better known in the literature as laser microanalysis or laser-induced breakdown spectroscopy, is a suitable method for the direct in-process measurement of elemental concentrations in various solid and liquid materials. This method has been developed recently by Krupp for in-process quality assurance and process control in different industrial branches such as steel production and plant making. As a result several LIESA instruments have already been developed or are under development for marketing. In all cases on-line and in-process elemental analysis of materials at various stages of production yield information on the quality of the material and the fabrication process. The beam of a pulsed high-power laser (irradiance: $1\times10^8$–$5\times10^9$ W cm$^{-2}$), focused onto the solid or liquid sample surface in an ambient gas atmosphere of normal pressure (focus area≈ablation area, 0.1–6 mm$^2$), produces a hot bright plasma (early electron temperatures, 20 000–30 000 K). The emitted plasma light is observed end-on and passes by way of an optical fibre bundle to a spectrometer, where it is detected in the focal plane by means of an optical multichannel analyser with high time resolution (on the microsecond scale). A fast computer evaluates the measured spectra and calculates the element concentrations *via* calibration procedures. Relative detection limits of between 10 and 100 ppm can be achieved for most of the detectable elements in various matrices (steel, rubber, rock and glass). Procedures are available to convert relative measurements with relative standard deviations of between 1 and 2% into absolute concentration values with relative accuracies of about 3%.

**Keywords:** *In-process laser microanalysis; remote surface analysis; depth profiling; laser ablation; optical emission spectrometry*



Laser ablation of solid or liquid samples and optical emission spectrometry of the microplasma produced is a simple and fast technique for direct elemental analysis. Time-consuming sample preparation can be omitted. Bulk and surface analysis in addition to depth profiling are possible with the same apparatus. Tight focusing of the laser beam even allows microanalysis of sample surfaces. Recently, two textbooks[1,2] have been published briefly describing the historical background and the present status of scientific investigations and applications. In the period 1989–1992 Niemax and co-workers[3–8] published a series of papers presenting systematic investigations of the spatial and temporal evolution of laser-produced microplasmas and ablation of the related material. By using a Q-switched Nd:YAG laser operating at its fundamental wavelength (1 064 nm) Niemax and co-workers found the following experimental conditions and parameters to be best-suited to laser-induced emission spectral analysis: (*i*) use of a buffer gas at reduced pressure (most appropriate, argon at 140 hPa); (*ii*) use of reduced laser irradiance (no electrical breakdown in the surrounding atmosphere when the sample is removed); (*iii*) use of long delay times (≥30 μs) between laser pulse and detector gate pulse; and (*iv*) use of analyte and reference spectral lines with comparable excitation energies.

A buffer gas plasma formed simultaneously with the ablation process serves as an energy reservoir for the atomization of ablated droplets and particles, and for the excitation of atoms and ions. The heating of the buffer gas plasma by inverse bremsstrahlung is most effective with argon. Since a buffer gas keeps ablated material in the observation region for a longer time and a larger fraction of this material can penetrate into the buffer gas plasma at reduced pressure, best analytical results were achieved with argon at 140 hPa. Recombination of the buffer gas plasma is completed after approximately 1 μs. At this time ablated material from the sample surface reaches the centre of the buffer gas plasma at almost supersonic velocities. Atomization and excitation processes start to develop. Complete atomization is achieved after 20–30 μs with number densities of free atoms and ions and plasma temperatures remaining high (>6 000 K). The buffer gas–sample material plasma can be described by partial local thermodynamic equilibrium verified by plasma temperature measurements using Boltzmann plots. Internal standardization can be applied and matrix independent measurements (common calibration graphs) can be performed when delay times greater than 30 μs and analyte and reference spectral lines of comparable excitation energies are used in optical emission spectrometry.

In 1986 Krupp started with basic investigations of the laser analysis method applied to solid and liquid steel samples (Carlhoff *et al.*[9]). A pilot system for on-line and in-process carbon and temperature monitoring was developed and successfully operated in a Krupp steel plant (Carlhoff and Kirchhoff[10]). This was the first successful attempt worldwide to install a laser-induced emission spectral analysis (LIESA) system in the harsh environment of a production steel plant. Meanwhile Krupp started the development of a laboratory prototype for the in-process monitoring of element distributions in polymeric materials (Lorenzen *et al.*[11]). Further activities in this field are the on-line control of geological raw materials on conveyor belts and investigations of depth profiling of multi-layers on metallic substrates.

The following sections describe the basics and some details of the different industrial LIESA applications at Krupp. Emphasis is placed mainly on instrument development rather than on fundamental scientific investigations.

## Instrumentation

The general set-up of all LIESA instruments is shown in Fig. 1. In some applications where element distribution measurements are performed, a linear scanner system is

*Presented at the 1992 Winter Conference on Plasma Spectrochemistry, San Diego, CA, USA, January 6–11, 1992.

**Table 1** Hardware components and ranges of operating conditions of LIESA instruments

| | |
|---|---|
| *Q-switched Nd:YAG laser—* | |
| Wavelength/nm | 1064 or 355 |
| Mode | Multimode |
| Pulse energy/mJ | 25–300 (on sample surface) |
| Pulse width/ns | 6–9 |
| Repetition rate/Hz | 10–25 |
| or | |
| *Excimer laser—* | |
| Wavelength/nm | 248 (KrF) |
| Pulse energy/mJ | 50–110 (on sample surface) |
| Pulse duration/ns | 26 |
| Repetition rate/Hz | 15–50 |
| *Optical multichannel analyser—* | |
| Detector | Gated MCP-intensified diode array (1024 pixel, UV enhanced) |
| Sensitive wavelength range/nm | 150–900 |
| Wavelength capture range/nm (see spectrometer) | 14–42 (in the UV) |
| Gate widths/$\mu$s | 0.2–10 |
| Delay times (laser gate)/$\mu$s | 0–30 |
| Data transfer speed/spectra per second | Maximum 50 |
| *Spectrometer—* | |
| Mounting | Czerny–Turner |
| Focal length/m | 0.5 ($f$/4) |
| Grating/rules per mm | 3600 or 2400 |
| Reciprocal dispersion/nm mm$^{-1}$ | 0.6 or 1.7 (in the UV) |
| Entrance slit-width/$\mu$m | $\leqslant$80 |
| *Linear scanner system—* | |
| Scan range/m | 0–1.2 |
| Scan velocity/m s$^{-1}$ | 0–2 |
| Scan acceleration/m s$^{-2}$ | 0–6 |
| Load/kg | 20 |

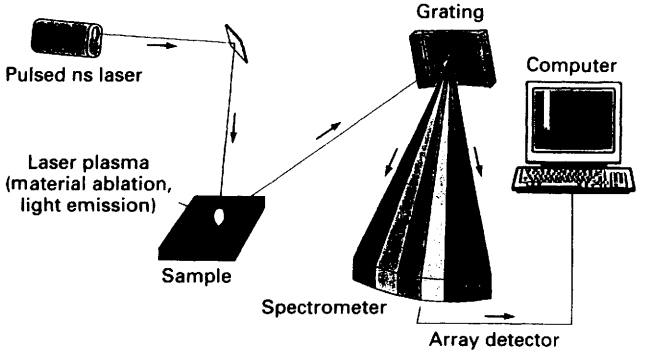


**Fig. 1** General set-up of LIESA instruments

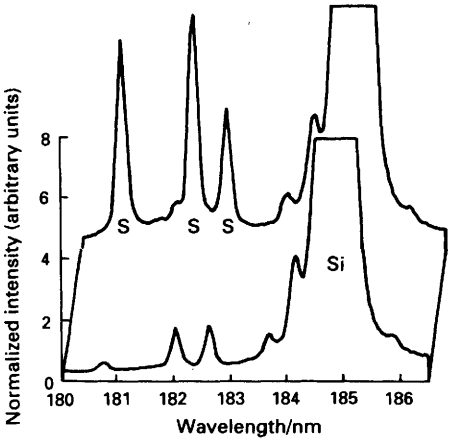


**Fig. 2** Comparison of detector signals in the spectral region 180–186 nm obtained with use of conventional optics (upper trace) and 3 m fibre optics (lower trace) from a rubber sample. The sulfur concentration is 1.12%

employed to scan the laser beam across the sample surface.

The specifications for the hardware components and the operating conditions are summarized in Table 1. Since the operating parameters are dependent on the application of the instrument, parameter ranges are given in most instances for reasons of simplicity.

When designing a LIESA instrument for a specific application special attention has to be paid to the selection of the appropriate laser system. Commercial Nd:YAG and excimer lasers were found to be most suitable for operation in industrial environments owing to their sturdiness and ease of operation. High pulse-to-pulse stability of both lasers [about 2% relative standard deviation (RSD)] and long lifetimes of the flashlamp of the Nd:YAG laser and of the gas fills and resonator mirrors of the excimer laser (up to $1 \times 10^8$ laser pulses in both cases) are additional features making these lasers useful for industrial applications.

In the next step the appropriate operating laser wavelength is most important to obtain the best analytical results. It was found that the 1024 nm Nd:YAG laser produces plasmas with strong emission on metallic and glass surfaces. Ultraviolet (UV) excimer laser wavelengths must be employed on polymeric surfaces since only then are sharp and regular ablation patterns produced without any thermal side-effects. For geological samples infrared

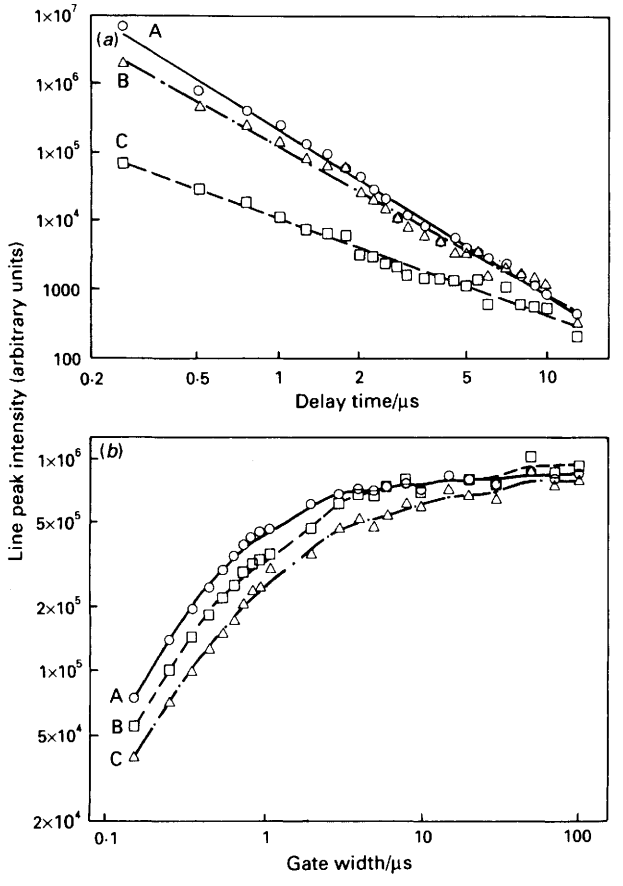


**Fig. 3** (*a*) Double-logarithmic plot of peak intensities of the lines: A, Si I 288.2 nm; B, Ca II 393.4 nm; and C, Al I 396.2 nm *versus* delay time. The gate width is always 200 ns. A rubber sample was used as the target. (*b*) Double-logarithmic plot of peak intensities of the lines: A, Mg II 279.6 nm; B, Mg I 285.2 nm; and C, Si I 288.2 nm *versus* gate width. The delay time is always 200 ns. A rubber sample was used as the target

(IR) as well as UV laser light give comparable analytical results.

Another key component in the LIESA instruments are the optical fibres used for guidance of the plasma emission light to the spectrometer system, thus greatly simplifying the opto-mechanical design and adjustment of the apparatus. The fibre output is directly coupled to the entrance slit of a 0.5 m spectrometer. It can be seen from Fig. 2 that the transmission of the fibre guide near the sulfur triplet rapidly decreases with decreasing wavelength (lower trace of Fig. 2) compared with the spectrum taken with direct lens imaging (upper trace of Fig. 2). The beam paths and spectrometer are purged with Ar and $N_2$, respectively. In addition, the cut-off transmission wavelength at about 180 nm is also governed by limited detector window transmission and detector sensitivity in addition to limited transmission through residual oxygen in the purged beam paths.

Transmission of nanosecond laser pulses through optical fibres with high peak power densities (>0.1 GW $cm^{-2}$) causes problems even with core diameters of up to 2 mm.

As described below, in some instances, element distribution measurements are performed. Here the laser beam is scanned across the sample surface by means of an optical system carried by a high speed scanning machine (single axis linear positioning stage). This industrial device is designed for long life under high duty cycle and continuous operating conditions. Linear drive actuation is effected by a brushless linear d.c. servomotor. Precision position feedback is achieved by an optical incremental linear encoder (for specifications see Table 1).

## Data Acquisition and Evaluation

The main component from the analytical point of view is the detection system connected to a host computer. The plasma emission light is detected with high time resolution. It is necessary to create a trigger signal coincident with the nanosecond laser pulse in order to start the delay and gate generator in the optical multichannel analyser. In the case of the Nd:YAG laser this trigger signal is directly available from the Q-switch electronics of the laser power supply, whereas in the excimer laser a fast UV sensitive photodiode mounted behind a laser beam aperture creates the trigger signal. A constant delay due to electrical propagation differences in the detector electronics always has to be taken into account when calculating the true delay time. As the laser analysis is restricted to atmospheric pressures in most instances, only delay times much shorter than 30 μs can be used. In general, the spectral line intensities decrease by at least two orders of magnitude within 3 μs after the nanosecond laser pulse [Fig. 3(*a*)]. Therefore, delay times must be kept short in order to obtain detector signals (count rates) with sufficient signal-to-noise ratio, particularly when taking spectra of single laser shots. In general, the width of the detector gate pulse should not be greater than 10 μs [see Fig. 3(*b*)].

Only two data acquisition modes are used throughout the measurements. Either the spectra are taken from each single laser plasma and transferred to the host computer or a certain number of spectra are taken from successive laser plasmas and then accumulated into one resulting spectrum. The first mode is used for measurements with a scanning laser beam while the second mode is used for measurements at a fixed sample position. When a certain loss of spatial resolution is acceptable during element distribution measurements, spectra accumulation can also be employed.

For the determination of net signals (central peak intensities of spectral lines), a mathematical procedure was developed. This model takes into account the underlying continuum radiation and the contributions of the wings of neighbouring spectral lines. Concentrations of analytes are determined *via* internal standardization. The ratio of net peak intensities of an analyte line to a reference line is found. The corresponding concentration ratio of the analyte to the internal standard is then calculated by using a calibration graph. However, owing to the limited wavelength range captured simultaneously by the detector array,

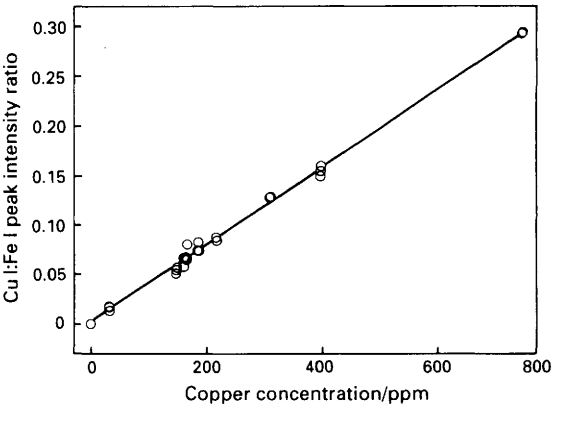


**Fig. 4** Calibration graph of copper (Cu I 327.4 nm) to iron (Fe I 327.1 nm) (in solid steel) peak intensity ratio *versus* copper concentration. Copper varies between 30 and 700 ppm in the certified reference samples

**Table 2** Selection of prominent analyte and reference lines used with LIESA for a variety of sample matrices

| | |
|---|---|
| *Solid/liquid steel in laboratory—* | |
| Analyte line | Si I 288.2 nm<br>Mn I 403.3 nm<br>Cr I 425.4 nm<br>Ni I 341.5 nm<br>Cu I 327.4 nm<br>C I 193.1 nm<br>Mo II 281.6 nm |
| Reference line | Fe I 439.4 nm |
| Reference element concentration | >90% iron |
| *Liquid steel in steel plant—* | |
| Analyte line | C I 193.1 nm |
| Reference line | Fe II 193.2 nm<br>Fe I 196.0 nm<br>Fe II 201.1 nm |
| Reference element concentration | >90% iron |
| *Rubber mixtures—* | |
| Analyte line | Si I 212.4 nm<br>Zn I 208.7 nm<br>S I 182.6 nm<br>Co II 228.6 nm |
| Reference line | C I 193.1 nm<br>C I 247.9 nm |
| Reference element concentration | ⩾80% carbon |
| *Geological samples—* | |
| Analyte line | Si I 288.2 nm<br>Al I 308.2 nm<br>Mg I 285.2 nm<br>Fe I 302.0 nm<br>Na I 589.0 nm |
| Reference line | Ca II 315.9 nm and lines of other elements |

a presumption of internal standardization, *i.e.*, comparable excitation energies of analyte and reference lines, cannot be fulfilled in many cases.

As an example, the linear calibration graph of the Cu I 327.4 nm:Fe I 327.1 nm line intensity ratio *versus* the copper concentration in the range between 30 and 700 ppm is shown in Fig. 4. The relative detection limit is around 10 ppm.

To achieve accurate absolute concentration measurements the most abundant element with a high concentration should serve as the internal standard. The prominent analyte and reference lines and the internal standards used with the different LIESA instruments are summarized in Table 2. The analytical figures of merit as a result of many experimental investigations are described in Table 3.

In order to determine absolute analyte concentrations either the concentration of the reference element must be known, or all elements must be measured relative to the reference element with unknown concentration. The latter can only be achieved when the major constituents of the sample are detected simultaneously in one spectrum. Then the sum of all concentrations is near to 100%. High concentration of the most abundant reference element significantly improves the accuracy of the absolute analyte concentration. In such cases the relative error of the analyte to reference concentration ratio is mainly governed by the relative error of the analyte concentration; relative accuracies of 3% are achievable when measuring absolute element contents (see Table 3).

All measurements should ideally be performed under constant operating conditions. However, in reality, changes in system parameters may occur from time to time, resulting in different plasma conditions (*e.g.*, temperatures and number densities). In such cases the measured calibration graphs are no longer valid. To overcome these problems and to allow for longer time periods between system recalibrations, the plasma conditions can frequently be monitored spectroscopically. In all spectral regions of interest atomic and ionic spectral lines of one element can be simultaneously detected. The intensity ratios of such atomic/ionic line pairs are a sensitive monitor of the averaged plasma temperature. By permanent observation of these intensity ratios, changes in plasma temperatures can be easily detected and a correction factor can be derived to calculate back to the plasma conditions for which the calibration graphs were measured (Carlhoff *et al.*[12]).

## Applications

### Direct Analysis of Liquid Steel

Steelmakers have long been searching for ways to obtain data on the condition of molten metal throughout production. Since conventional methods such as lance sampling lead to an interruption of the process there is a strong need for on-line control. By using laser-induced emission spectrometry it is possible to determine directly the concentration of chemical elements in the melt. A LIESA instrument has been adapted to an 80-t AOD (argon–oxygen decarburization) converter at a Krupp steel plant in Germany. This system measures the carbon content (by laser analysis) and the temperature of the melt (by pyrometry). Additional laboratory measurements were carried out at the University of Madrid.

**Table 3** Analytical figures of merit. In most cases ranges are given to cover all investigated applications of laser-induced emission spectral analysis

| | |
|---|---|
| On-line capability | Detection, transfer and partial evaluation of a maximum of 50 single spectra per second (1 spectrum per laser shot for 1 024 14-bit integers) |
| In-process capability | Direct elemental analysis, simultaneous multi-element analysis, no sample preparation, access to targets in harsh and hazardous industrial environments |
| Micro/macro sampling (Nd:YAG, excimer laser) | Ablated masses of 0.1–7 $\mu$g per laser shot, ablation areas of 0.1–6 mm$^2$, linear scanning of maximum 2.5 m s$^{-1}$ scan velocity |
| Relative detection limit | 10–100 $\mu$g g$^{-1}$ |
| Absolute detection limit | 1–100 pg |
| RSD value | 1–2% |
| Relative accuracy | 3% |
| Dynamic range | Linearity over 1–3 orders of magnitude |

**Fig. 5** Water-cooled box at converter wall containing laser head, optics and control electronics

The system design for the converter is as follows: the beam of a high-power Nd:YAG laser (wavelength, 1 064 nm) is focused onto the surface of the melt through a narrow channel in the side wall of the converter. Pre-heated argon gas ($T > 800$ °C) is injected to prevent the steel from escaping and the melt at the end of the channel from solidifying. The laser beam produces a hot plasma. The light generated passes by way of a 7.5 m long optical fibre to the spectrometer where it is detected with an optical multichannel analyser (see above).

A computer is used to calculate the concentrations of the elements from the detected spectral lines. Melt temperatures are determined by a pyrometer. The results are transferred to the process computer for optimum production control.

To achieve correct alignment of the laser beam through the converter channel it was necessary to attach laser head and beam guiding optics directly to the converter wall. These parts of the system are installed in a closed, water-cooled box (Fig. 5) while the remaining parts (host computer, electronic control units, spectrometer, laser power supply and gas handling system) are contained in a housing on the converter platform.

During many runs, the LIESA system proved that it can sustain the extreme environmental conditions of a steel production furnace.

The system has been operated at the converter for several months. A set of spectra from liquid steel in the near vacuum UV spectral region with the 193.1 nm carbon analyte line at different carbon concentrations is shown in Fig. 6. All remaining lines are atomic and ionic iron lines. By accumulating the optical emission of 200 laser shots within 10 s, repeatability is significantly improved. Despite the very small observation angle and the long optical path of the plasma light, which has to pass several mirrors, lenses

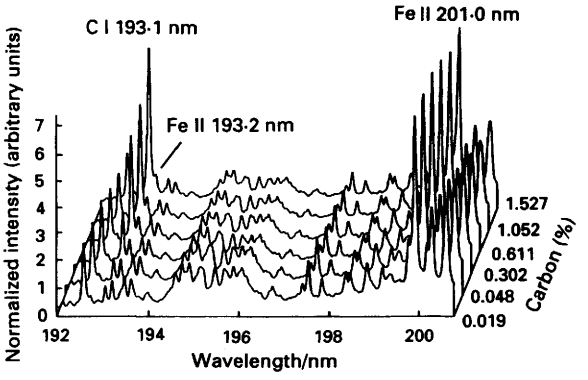


**Fig. 6** Spectra of liquid steel with increasing carbon content. The signal intensities are normalized to the Fe II 193.2 nm line. The carbon analyte line at 193.1 nm and one of the iron reference lines at 201.0 nm are indicated

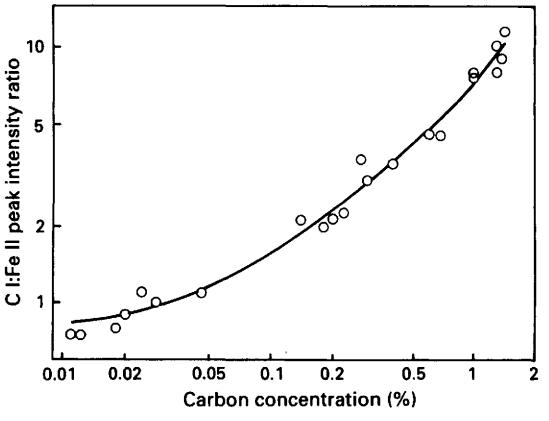


**Fig. 7** Calibration graph of carbon (C I 1931 nm) to iron (Fe II 193.2 nm) (in liquid steel) peak intensity ratio *versus* carbon concentration

and the optical fibre, resolution and signal-to-noise ratio of the resulting spectra are excellent.

The concentration of carbon can be evaluated by calculating the net line peak intensity ratio of the carbon line to an isolated iron line as internal standard. A calibration graph for the decarburization as a result of several melts is shown in Fig. 7. After lance sampling, carbon concentrations could be measured off-line in the analytical laboratory with X-ray fluorescence. At very low carbon contents the graph flattens because of coincidence with a small iron line. The carbon detection limit from this graph is less than 200 ppm. It will be possible in the near future to avoid occasional solidification of metal in the converter channel by optimizing the argon gas pre-heating process.

The application of LIESA to the converter will permit optimum control of the melt process. Thus, tap-to-tap times can be shortened, reducing consumption of gases, fluxes and refractories. This will enhance cost efficiency in steelmaking. More accurate adjustment of the composition will improve steel quality. The LIESA system appears to be suitable not only for the converter process but also for other components in a steel production line.

## Homogeneity Measurements of Tyre Rubber in the Mixing Shop

The European tyre industry is today faced with two major trends: a constant growth in raw materials being processed and a decrease in profit compared with previous years.

Since the market rigorously demands low price and high quality, there are various approaches that can be used to improve profitability. The reduction of material costs is limited owing to their close relation to product performance. However, processing techniques offer a number of possibilities for higher economy. Increased productivity and improved consistency of quality can be achieved by better preparation and performance during the compounding stages. The tolerances in compounding and mixing must be kept as tight as possible so that the rejection rate is decreased to a minimum. Additionally, automation must be increased in order to reduce the human influence on the result.

For industrial rubber mixing processes, it is desirable to evaluate on-line the dispersion of the different ingredients in the polymer matrix (*i.e.*, compound homogeneity). Therefore, Krupp, Pirelli (as a tyre manufacturer) and King's College London (as a scientific supporter) started the development of a laboratory system capable of in-process monitoring of the homogeneity of rubber slabs in the open mill and other locations in the early stage of tyre production.

By scanning the focused beam of a pulsed excimer laser across the surface of rubber slabs in a rubber mixing line, spatial element distributions can be measured and evaluated on-line. Thus, the actual element composition and homogeneity of the rubber material can be monitored frequently during the mixing and forming process. Each laser pulse produces a hot bright plasma on the rubber surface in a buffer gas flow of constant flow rate (argon at normal pressure). The optical plasma emission is detected and the spectra are evaluated as described above.

Systematic investigations of the optical plasma emission were performed in the wavelength region from 180 to 800 nm. All measured spectral features in that range could be identified and assigned to appropriate elements and molecules. Atomic and ionic spectral lines of C, H, S, Si, Zn, Co, Mg, Al, Ca, Na and K and molecular bands of $C_2$ and CN have been detected. The temporal behaviour of the laser-induced plasma under different experimental conditions has been studied. It has been observed with tyre rubber that spectral line peak intensities exhibit roughly the same behaviour as the lines of all the other materials analysed [see Fig. 3(*a*) and (*b*)].

The interaction of the UV laser with rubber was also investigated in detail. As expected the UV laser ablation pattern on the rubber surface exhibits sharp edges without thermal side-effects. This is not the case with the IR Nd:YAG laser beam. Excimer laser peak powers as low as $1 \times 10^8$ W cm$^{-2}$ were sufficient to produce plasmas with strong spectral emission. Ablation depths of 2 $\mu$m per laser pulse with an ablation area of 3 mm$^2$ have been achieved with this irradiance employing the KrF excimer laser at 248 nm.

A typical calibration graph is shown in Fig. 8 where the line peak intensity ratio of a zinc to a carbon line is plotted *versus* the zinc oxide to carbon concentration ratio. Such calibration graphs reveal RSD values of between 0.5 and 2%. The corresponding spectra are shown in Fig. 9. Since each spectrum is normalized to the C I 193.1 nm line, variations in the sulfur and silicon (oxide) content of the rubber samples can also be seen.

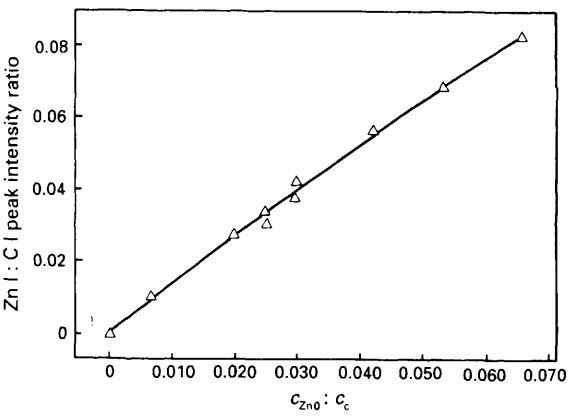


**Fig. 8** Calibration graph of zinc oxide in solid tyre rubber. The peak intensity ratio of the Zn I 208.7 to the C I 193.1 nm line is plotted *versus* the zinc oxide to carbon concentration ratio

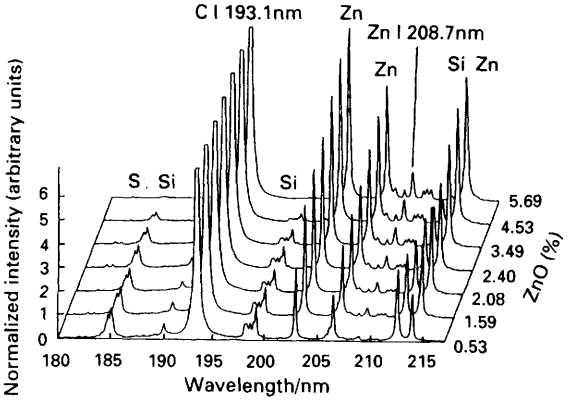


**Fig. 9** Spectra of solid tyre rubber with increasing zinc oxide content. The signal intensities are normalized to the C I 193.1 nm line. The zinc analyte line at 208.7 nm, the carbon reference line at 193.1 nm and spectral lines of S and Si are indicated

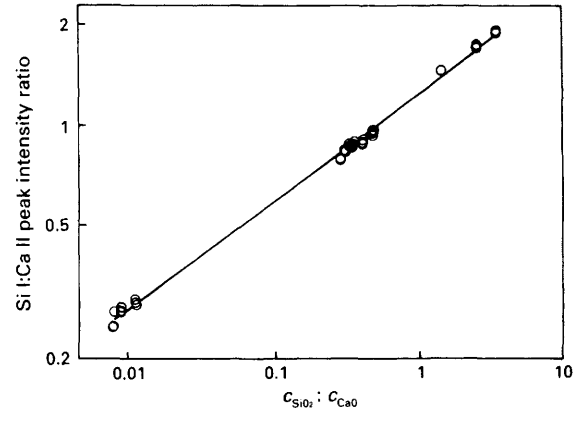


**Fig. 10** Calibration graph of silicon oxide in geological samples. The peak intensity ratio of the Si I 288.2 to the Ca II 317.9 nm line is plotted *versus* the silicon oxide to calcium oxide concentration ratio

## Element Distribution Measurments of Geological Materials on Conveyor Belts

There is a great need in industry for the on-line control of continuous mass streams of geological raw materials. By permanent monitoring of element distributions, raw materials with narrow composition tolerances can be available ahead of further processing. In the case of bad or incorrect compositions, measures will be taken to reject or divert the materials that are outside of the range of tolerance.

Preliminary studies of different samples led to encouraging results. A calibration graph of $SiO_2$ *versus* CaO employing the Si I 288.2 nm analyte and Ca II 317.9 nm reference line is shown in Fig. 10. Several data points lying close together at a given concentration ratio demonstrate the very good precision of the measurements.

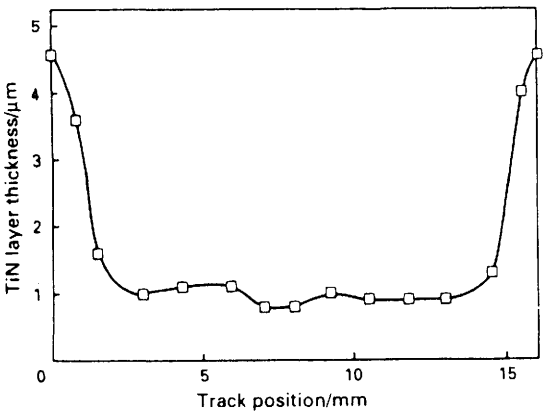


**Fig. 11** Thickness profile of TiN coated on a flat metallic substrate along a linear track on the sample surface

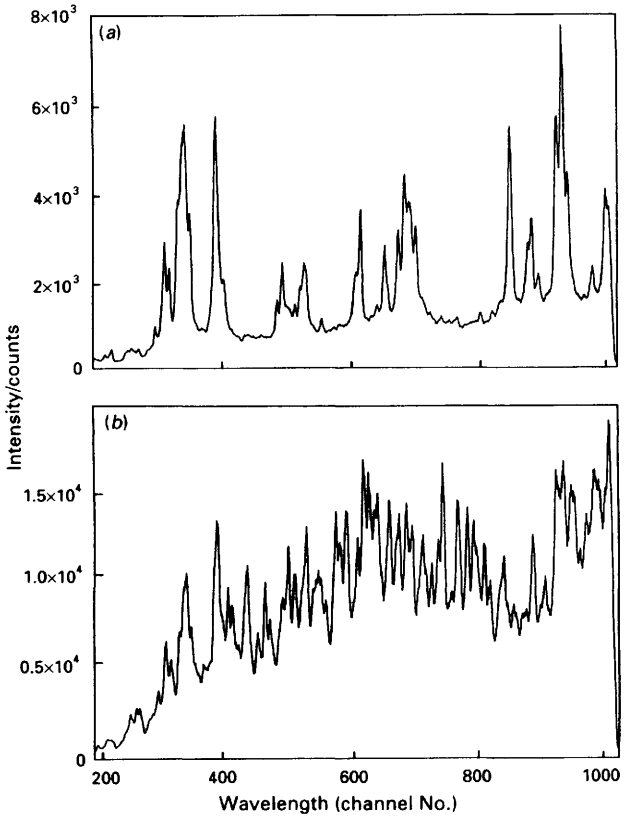


**Fig. 12** (*a*) Spectrum of Ti in the UV spectral region emitted after the tenth laser pulse and (*b*) spectrum of the metallic substrate in the same spectral region as in (*a*) emitted after the hundredth laser pulse

### Depth Profiling of Muilti-layers on Metallic Substrates

Intensive investigations at Krupp showed that laser analysis is not only suitable for elemental analysis but also for the depth profiling of coated substrates.

During laser–matter interaction, material is ablated in a defined way. The ablation pattern and ablation depth per laser pulse can be controlled *via* the laser parameters (spatial intensity distribution of the laser beam, pulse energy, pulse repetition rate and shape and size of laser focus). If each laser plasma is analysed a depth profile of the substrate layer(s) is created. The change in a layer is indicated by the change in the detected spectral pattern.

A thickness profile (single TiN layer on a metallic substrate) along a straight line on the flat surface of the coated sample is shown in Fig. 11. The ablation depth of the pulsed laser was 0.1 μm per pulse. Corresponding spectra are presented in Fig. 12(*a*) and (*b*) (same wavelength region in the UV). A Ti spectrum emitted after the tenth laser pulse is shown in Fig. 12(*a*) while a metal spectrum emitted after the hundredth laser pulse deep in the substrate can be seen in Fig. 12(*b*). The measured profile was in excellent agreement with results of off-line standard measurement techniques.

## Conclusions

Laser-induced emission spectral analysis appears to be a very promising method for on-line analysis in those industrial fields where element distribution measurements of materials at all stages of production yield information on the quality of material and production process. At present Krupp is developing a whole family of LIESA instruments to cover the needs of different industrial branches.

Financial support for the development of the LIESA systems by the German Minister of Research and Technology (BMFT), by the European Communities for Steel and Coal (ECSC) and by the BRITE/EURAM programme of the Commission of the European Communities is gratefully acknowledged.

## References

1 Moenke-Blankenburg, L., *Laser Microanalysis*, Wiley, New York, 1989.
2 *Laser-Induced Plasmas and Applications*, eds. Radziemski, L. J., and Cremers, D. A., Marcel Dekker, New York, 1989, pp. 295–346.
3 Ko, J. B., Sdorra, W., and Niemax, K., *Fresenius' Z. Anal. Chem.*, 1989, **335**, 648.
4 Leis, F., Sdorra, W., Ko, J. B., and Niemax, K., *Mikrochim. Acta*, 1989, **II**, 185.
5 Sdorra, W., and Niemax, K., *Spectrochim. Acta, Part B*, 1990, **45**, 917.
6 Niemax, K., and Sdorra, W., *Appl. Opt.*, 1990, **29**, 5000.
7 Sdorra, W., and Niemax, K., *Mikrochim. Acta*, 1992, **107**, 319.
8 Sdorra, W., Brust, J., and Niemax, K., *Mikrochim. Acta*, 1992, in the press.
9 Carlhoff, C., Lorenzen, C.-J., Nick, K.-P., and Siebeneck, H.-J., in *In-Process Optical Measurements*, ed. Spring, K. H., *Proc. SPIE*, SPIE Publications, Bellingham, vol. 1012, 1989, pp. 194–196.
10 Carlhoff, C., and Kirchhoff, S., *Laser Optoelektronik*, 1991, **23**, 50.
11 Lorenzen, C.-J., Jogwich, M., Burge, R. E., Michette, A. G., Daghooghi, R., and Nahmias, M., paper presented at the BRITE/EURAM-EUREKA Workshop on Polymer Technology and Industrial Applications, Ferrara, Italy, May 13–15, 1991, Book of Abstracts 2, pp. 122–125.
12 Carlhoff, C., Lorenzen, C.-J., and Nick, K.-P., German patent No. DE 39 11 965 C2; date of application: April 12, 1989.

*Paper 2/00713D,*
*Received February 11, 1992*
*Accepted April 13, 1992*